

# Scientific CMOS Camera for Observation of Dim Space Objects

Michael Jacox, David Breckon, Paul Sikangwan, Joshua Villafior  
Space Micro Inc, San Diego, CA

## 1. ABSTRACT

This paper describes modeling and comparison of several candidate imagers for space based observation of sunlit objects. A camera designed for long term space operation using a scientific complementary metal-oxide-semiconductor (sCMOS) imager sensor is presented. sCMOS image sensors can offer extremely low noise, rapid frame rates, wide dynamic range, high quantum efficiency, high resolution, and a large field of view in one image. This makes them well suited for high fidelity low-light-level conditions from space platforms. A detailed camera model was developed to compare candidate imager sensors that included optical, imager and environmental parameters. Camera level trade studies include an assessment of Minimum Detectable Irradiance (MDI) versus aperture, exposure time and camera platform angular rates. The results demonstrate the advantages of extremely low read-noise and high quantum efficiency imagers for space based observation of space objects. The camera design is optimized based on the sCMOS features for the harsh space radiation environment.

## 2. SCIENTIFIC CMOS IMAGER

Scientific Complimentary Metal Oxide Semiconductor (sCMOS) is a term that refers to CMOS imagers with high sensitivity and very low noise. The combination of high sensitivity and low noise ensures high signal-to-noise ratio during low-light imaging and makes these devices obvious candidates for stellar cameras. These image sensors have pixels composed of a photodiode and an amplifier that converts charge into voltage. The voltage of each pixel is output by turning on the switch one by one, and the data of each horizontal line is read by the on-chip column amplifier and A/D in parallel and simultaneously. This results in very fast readout speed while keeping the readout noise very low. This combination of features is attractive for several scientific fields of imaging investigation and hence the term scientific CMOS. There are several suppliers of sCMOS imagers including Hamamatsu and Fairchild Imaging (now BAE Systems). This paper is about the modeling and camera design incorporating the BAE Systems CIS2521F large format imager.

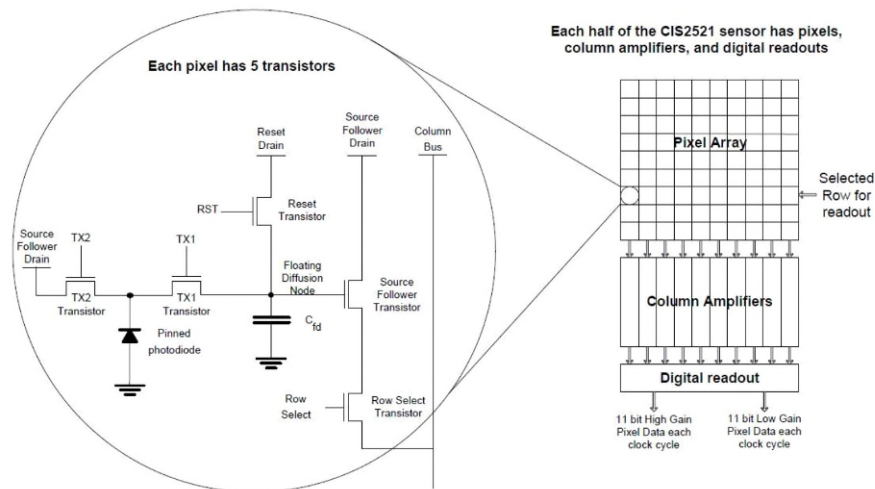


Figure 1. The BAE Systems sCMOS Imager Block Diagram [1].

The CIS2521F is a large format, ultra-low noise CMOS image sensor intended for applications requiring high quality imaging under extremely low light conditions. The device features an array of 5 transistor (5T) pixels on a  $6.5\mu\text{m}$  pitch with an active imaging area of 2560(H) x 2160(V) pixels as depicted in Fig 1. The CIS2521F delivers

extreme low-light sensitivity with read noise less than 2 electrons RMS, Quantum Efficiency (QE) above 55% and very low dark current. The sensor runs in Rolling and Global Shutter readout modes. The sensor has two ADC channels per column with one optimized for low light levels and the other optimized for high light levels, enabling high dynamic range data collection in a single image. The sensor supports user programmable row start/stop control for region of interest (ROI) readout. The sensor is housed in a 168-pin ceramic leadless chip carrier package which provides good stability over a wide temperature range. The comparison of this sensor versus legacy devices and other imagers will be discussed in the following sections.

### 3. CAMERA MODEL

Space Micro has developed a MATLAB camera model that incorporates the parametric details of the system and allows a variety of trade studies to be performed. The model includes intrinsic properties of the imager, the optics of interest, the signals of interest including background, and the operational parameters.

The intrinsic imager properties taken into account with the camera model include; exposure time, quantum efficiency, fill factor, pixel size, dark current, read noise, Analog-to-Digital-Conversion (ADC) bits, ADC voltages, gain settings, and gain offset settings. The read noise and dark current parameters are often known as a function of temperature and radiation dose.

The optical parameters adjusted in the model include an estimate of stray light noise added to the imager and lens parameters that include; field of view (FOV), entrance pupil diameter (EPD), point spread function (PSF), and spectral dependent transmissivity. Often the model is used to estimate the requirements for the lens design.

The source signals of interest in the model are the minimum detectable irradiance (MDI) for the spectrum of application. The model also has provisions for adjusting the background signals related to solar system sources and galactic light. The target irradiance and centroid accuracy can be predicted parametrically using this model.

The operational parameters of interest include the angular rotational rates or line of site (LOS) rates and the desired signal to noise ratio (SNR) to be used. These parameters are adjustable based on mission application of interest.

An illustration of the model prediction of detectable star magnitude versus FOV, MDI versus LOS rate and the probability of detected solar illuminated objects are shown in Fig 2 below. The modeling shown used the OnSemi HAS2 CMOS Active Pixel Sensor (APS) [2] that has been the baseline for Space Micro star tracker units and space cameras. As shown in the figure each of the key parameters can be traded against the possible range of design choices to help optimize a system.

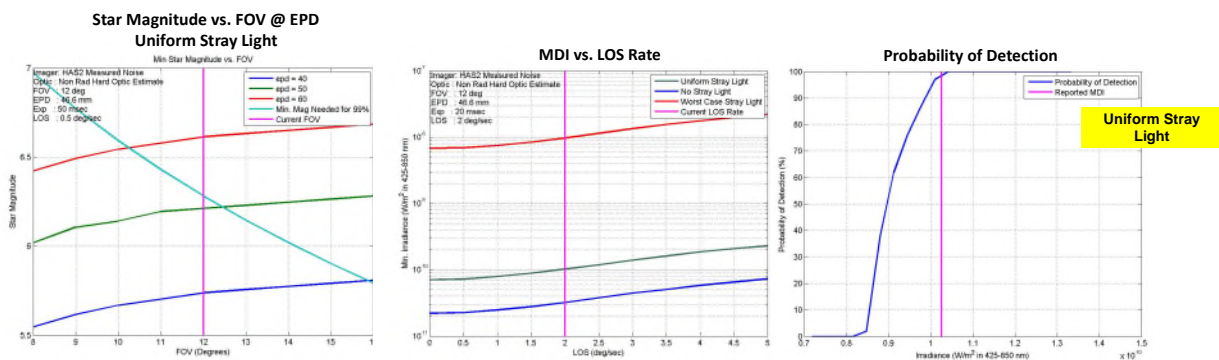
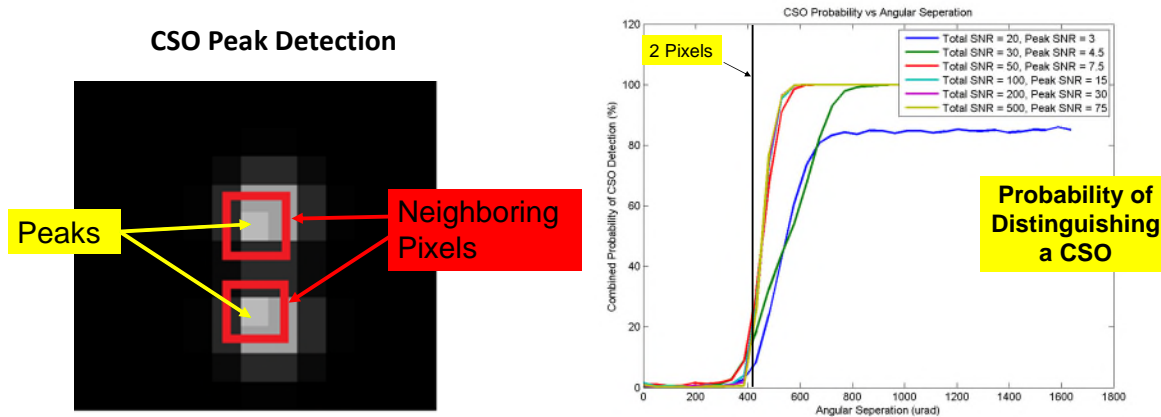


Figure 2. Benchmarked Camera Model Useful for Key Trades

Additionally, the camera model can be used to assess the ability to distinguish closely spaced objects (CSO) given the predicted irradiance, PSF and expected angular separation of the objects. The CSO peak detection assumes neighboring pixels are less on all four sides. Results of CSO analysis available within the camera model are illustrated in Fig 3 below. The probability of detecting CSOs of various angular separations is plotted for a variety of SNR operating regimes.



**Figure 3. Camera Model Allows Estimate of Detection of Closely Space Objects**

Another important trade for observing dim space objects involves the camera dynamic range in the presence of realistic backgrounds that include stray light (unwanted solar illumination not rejected by the camera baffle). Estimates of stray light levels on the imager are made with separate optical analysis tools such as ZEMAX or CODE V. In order to understand the dynamic range of a CMOS imager the pixel well, amplifier, and ADC architecture must be modeled. The illustration in Fig 4 shows the assumptions used for modeling the imager response while the plots provide the summary of dynamic range versus exposure time for a variety of gain settings. The results depicted in Fig 4 include uniform stray light and an LOS of 2deg/sec.

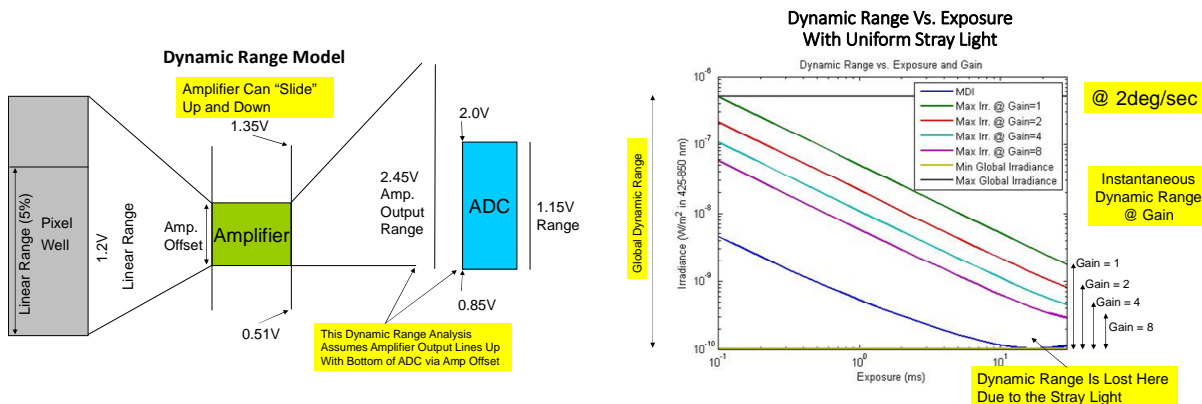


**Figure 4. Dynamic Range Modeling Leads to Valuable Trades**

The camera model has been useful in developing the Space Micro product line including the uSTAR-200M, the Miniature Integrated Star Tracker (MIST), the 4K Space Camera, and the new 5MP Space Camera. The baseline star tracker product has been the uSTAR-200M which uses the HAS2 imager from OnSemi. However, several years ago the vendor announced the product was discontinued and its replacement the HAS3 has not yet been available for demonstration or purchase. So, Space Micro has been investigated alternative solutions for both a star tracker and space camera capable of spotting and centroiding dim objects.

#### 4. IMAGER COMPARISON AND MODELING RESULTS

The space camera modeling has illustrated that for dim objects and modest exposure times of 10s of milliseconds a key requirement is low read noise. The objective of the comparison described in this section is to evaluate the sCMOS image sensor against the existing HAS2 and one of the better performing CCD imagers produced by MIT Lincoln Labs the CCID-88.

The parameters for each of the imagers is summarized in the Table 1 below.

**Table 1. Imager Properties**

Imager Property	HAS2	CCID88	CIS2521
Pixels	1024 x 1024	2068 x 1044	2560 x 2160
Pixel Size	15 microns	15 microns	6.5 microns
Read Noise	55 electrons (@ 22C)	12 electrons (@ -40C)	2 electrons (@ 22C)
Quantum Efficiency (QE)	45% @ 600nm	90% @ 600nm	55% @ 600nm
Dark Current	20e <sup>-</sup> /pixel/sec @ 22C	20e <sup>-</sup> /pixel/sec @ -40C	35e <sup>-</sup> /pixel/sec @ 20C
Linear Full Well	100,000 e <sup>-</sup>	100,000 e <sup>-</sup>	30,000 e <sup>-</sup>

The first modeling results compare the three imagers; the HAS2, the CCID-88 and the CIS2521 for exposure time versus MDI without stray light influences. The model used the same optical and background assumptions for all three imagers. As illustrated in Fig 5 below the HAS2 is the least performer for exposure times in the range of 10 to 100 msec. The MIT LL CCD imager is much better than the HAS2 but not as good in MDI performance as the CIS2521. This is due primarily to the lower read noise of the sCMOS device despite the quantum efficiency of the CCD being considerably better. This result is interesting for dim objects because it illustrates that QE is not the driving factor for performance if exposure times are on the order of less than 100 msec.

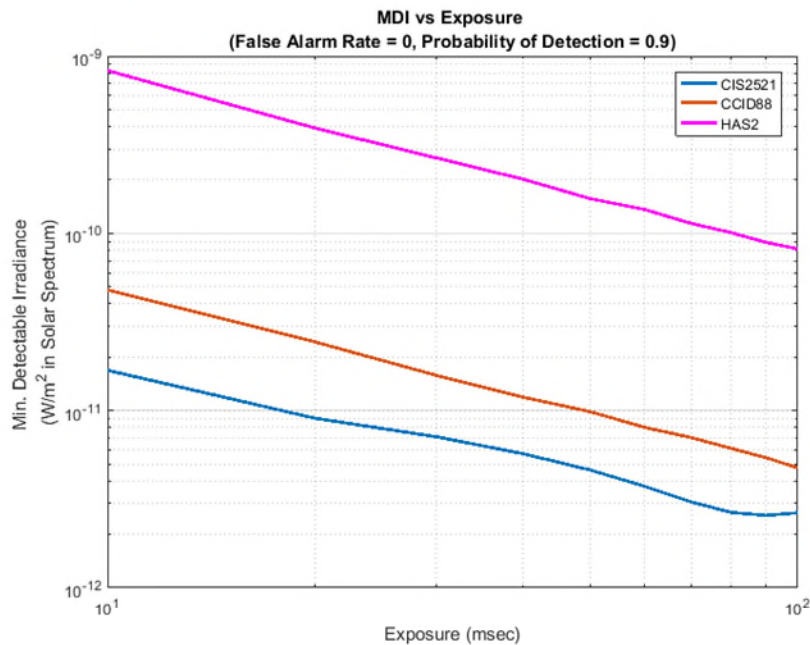


**Figure 5. Sensitivity Comparison for CCD, CMOS and sCMOS Cameras**

While it becomes clear that the read noise dominates the MDI for several imager candidates it isn't clear what the impact on centroid accuracy would be. We ran a number of simulations with varying parameters to understand the comparison of the CCD and sCMOS sensors for centroid accuracy. The results are depicted in Fig 6 below. At a star magnitude of about 5 mv the centroid errors for the CCD and sCMOS are very close (< 0.03 pixels). The limiting factor for the CCD is read noise but the limiting factor for the sCMOS is shot noise. It is important to note that these are not being compared at the same temperature. The CCD is presumed operating in a camera with a focal plane temperature of -40C while the sCMOS performance assumes room temperature operation.

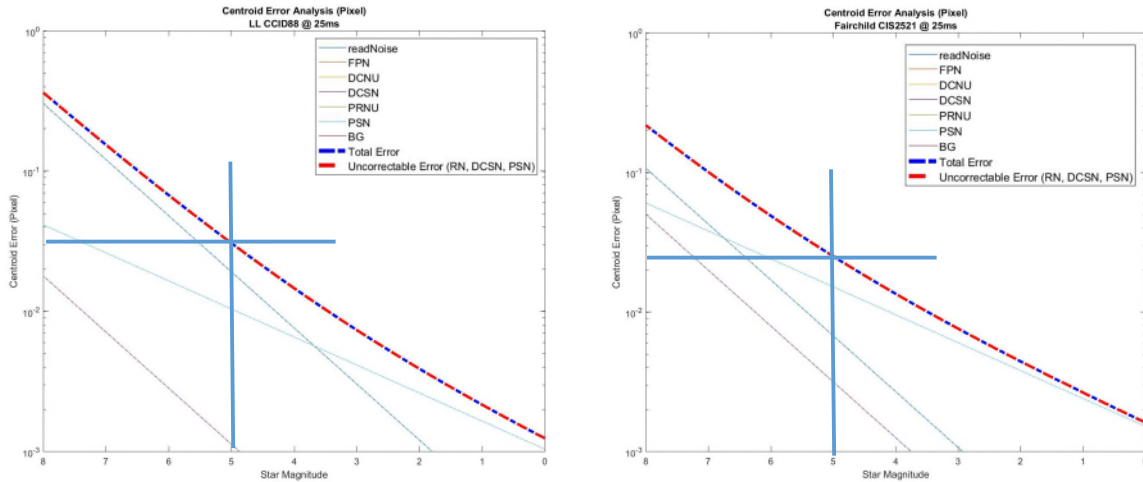


**Figure 6. Comparison of Centroid Errors for CCD and sCMOS Cameras**

Assessing the impact of the lower read noise of the sCMOS imager compared with the higher QE of the CCD another parameter is evident. The CCD imager has a lower dark current that comes into play at higher exposures times beyond those typical of a star tracker. However, for cameras looking for very dim objects very long exposures might be necessary and hence the CCD might begin looking better. For our purposes we assume that with sufficient registration accuracy we could stack many short exposure frames to achieve the same effect of very long exposures.

## 5. SCIENTIFIC CMOS CAMERA DESCRIPTION

Space Micro has recently completed qualification and acceptance testing of the uSTAR-200M cameras for use as start trackers and in some cases space situational awareness cameras. The photos of these flight units are provided in Fig 7 below. All of these have used the HAS2 imager. Now, Space Micro has introduced a newer version of both the star trackers and space cameras that will use the sCMOS imagers. The trade studies have led us to the conclusion that the very low read noise and robust features of the CIS2521F are best suited for a new set of space camera products.

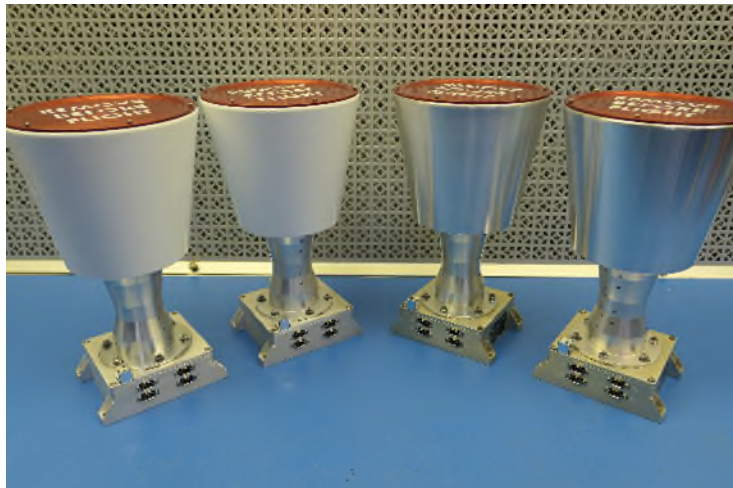


**Figure 7. Space Micro has Recently Delivered Flight Units as Star Trackers and Space Cameras**

Our baseline space camera product is designed to be minimal SWaP but also modular to adapt to varying mission applications. For example, the base camera housing includes the imager and control electronics as well as the high speed interface to a spacecraft over Spacewire or CameraLink data channels. Redundant power and data connectors

allow the camera to be cross-strapped for missions that require redundancy. The lens assembly can be altered for FOV and EPD but still mate with the camera housing. The lens is composed of radiation hard glass elements and provisions are made for venting between elements to eliminate pressure differential from launch ascent into space vacuum. The baffle can be replaced based on stray light requirements and the FOV. Each camera assembly includes a precision optical cube for customers to align the boresight relative to the cube. The illustration of the camera design is provided in Fig 8 below.

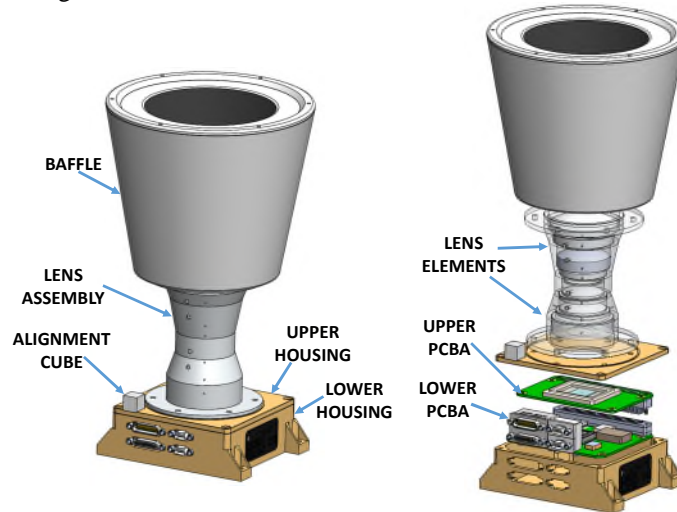


**Figure 8. Scientific CMOS Camera Illustration**

The electronics for the new camera are enhanced relative to the baseline camera in several ways. First, the sensor board is physically separated from the processing board to allow for modular testing and screening as necessary. The separate configuration allows for replacement of the imager when the value of a device warrants a change. The electrical board stack-up is depicted in the Fig 9 below. Each of the boards is designed to meet the IPC Class 3 standards and the parts are selected at a level needed for the mission from Commercial Space parts grade to NASA EEE-INST-002 compliant components.

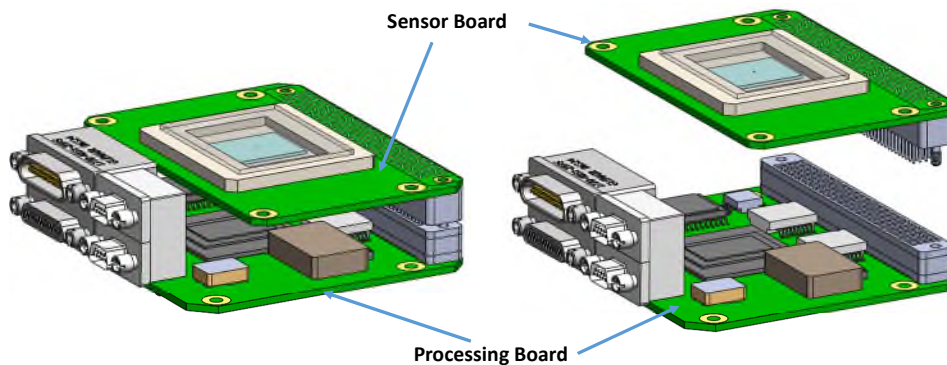


**Figure 9. Modular Design Allows for Sensor Board Upgrades**

The electronics functional block diagram is depicted in Fig 10 below. The sensor board includes a high speed connection to the processor board through a stacking connector. Voltage regulation and passive components are on the Sensor board. The processing board employs a Zynq hybrid device with radiation mitigation features included for rapid restart and fault trapping in the software and firmware. The electronics are also capable of providing the quaternion out solution over the Spacewire interface without additional external processing. The dual processor and FPGA fabric of the hybrid device also allow for image processing to be conducted on the space images and higher level data reported to the spacecraft.

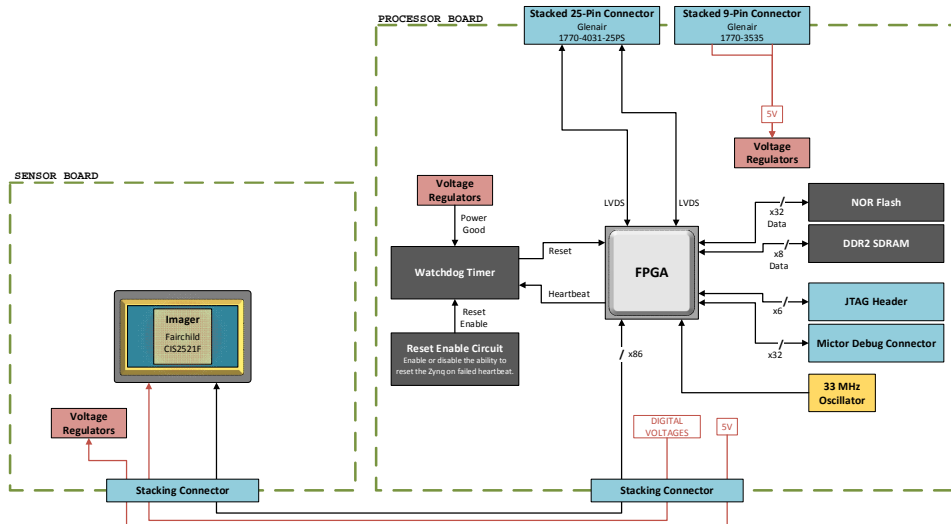


**Figure 10. Scientific CMOS Camera Electrical Functional Block Diagram**

The mechanical features of the sCMOS camera are critical for surviving the launch environment and operating over often large temperature ranges. The structural modeling techniques of the camera have been validated on the flight units previously delivered. The random vibration and shock environments used are selected to envelope a reasonable range of interest. The analysis starts with a detailed finite element model of the camera system including the base housing, lens assembly and baffle. The results of the random vibration and shock analysis are depicted in Fig 11-12 below. Locations of highest stress are identified and reviewed to ensure adequate margin exists or that changes need to be made to accommodate the peak stress or predicted deflection.

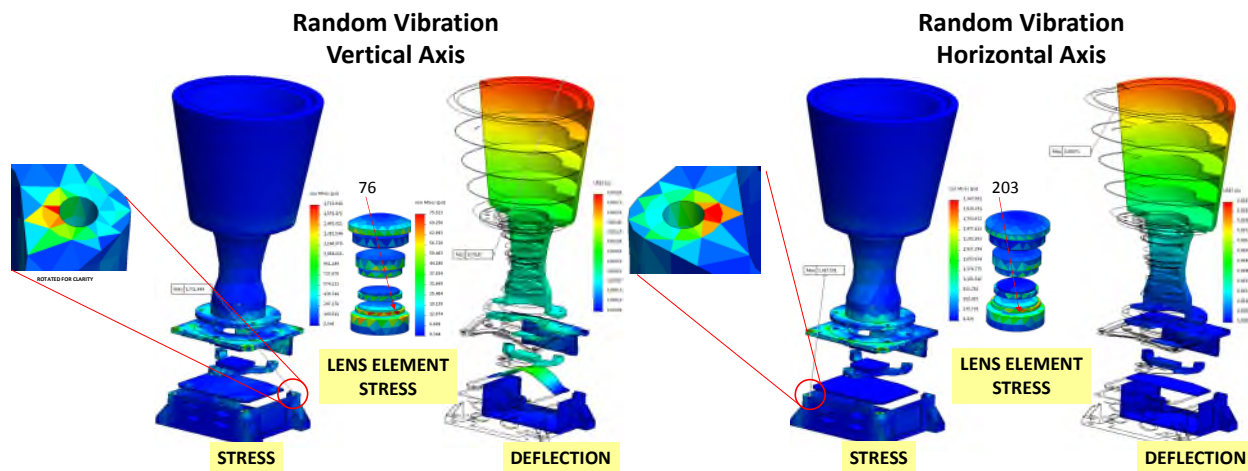


**Figure 11. Vibration Analysis Illustrates Adequate Strength Margins**

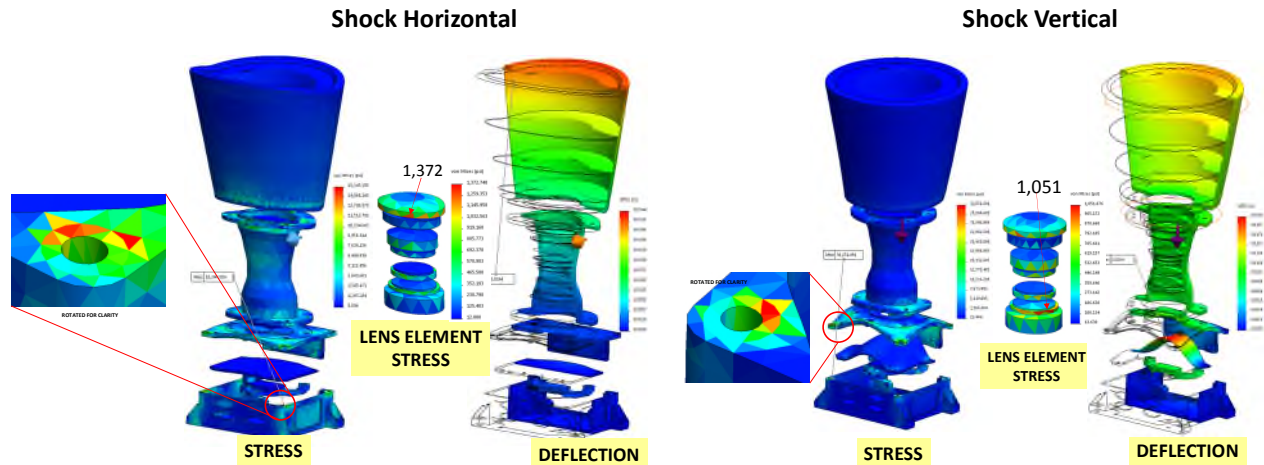


**Figure 12. Results of Shock Analysis Demonstrate Design Margin**

The design approach for meeting difficult thermal ranges on orbit is to use the baffle for heat rejection from the imager. This technique requires modeling of the radiant heat exchange with the sun at various orientations. The worst case conditions include the sun energy normal to the camera boresight and the Earth albedo entering the baffle FOV. The nominal baseplate or mounting interfaces are selected to be from -34C to +61C. We expect this range to be sufficient for the majority of mission applications. The imager is passively cooled with conduction from the shimming tripod to the baffle exterior. Varying baffle thermal treatments/paints can be used depending on the mission parameters. The dark frames for the imager at differing temperature ranges are stored on the processor board. The results for both cold and hot cases in illustrated in Fig 13 below. Sufficient margin exists in both extremes to allow for long life operation of the imager and electrical components.

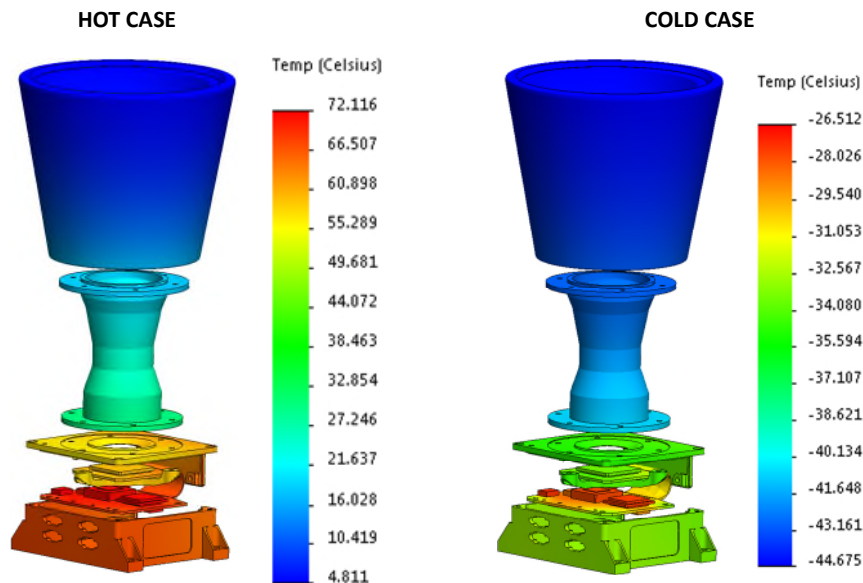


**Figure 13. Thermal Modeling Indicates Sufficient Temperature Margin.**

The space camera mechanical analysis has been completed to verify that launch vibration, shock and thermal cycling extremes will not result in reduced life or failure of key components. The benchmarking of these analysis has been completing through recent qualification testing of the design.

## 6. RADIATION TESTING OF sCMOS IMAGER

Space Micro has already begun an IRAD effort to complete SEL threshold testing of the baseline Fairchild (BAE) sCMOS imager. The objective of the testing is to establish the probability distribution or cross section for single event effects that require power reset or result in failure. Various test facilities and beam stopping configurations have been assessed and it was determined that tests will be performed at Texas A&M University cyclotron facility in 2018. Stopping and Range of Ions in Matter (SRIM) have been conducted to define the heavy ion cocktail to be used at the TAMU cyclotron.

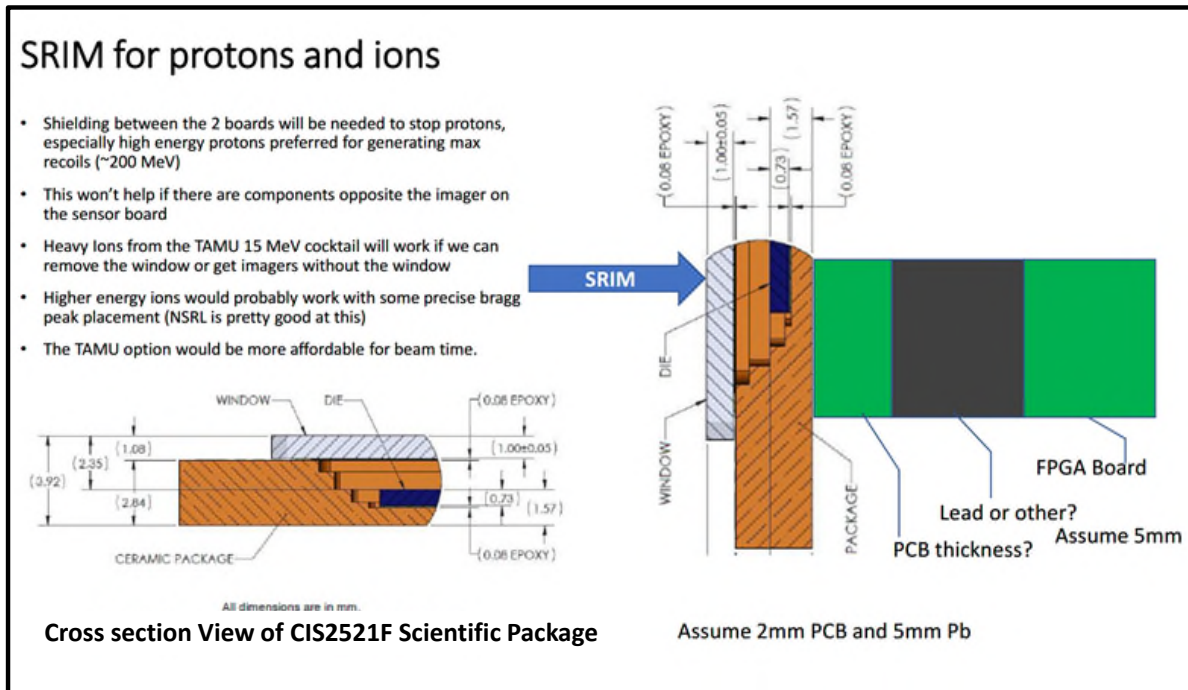


**Figure 14. Heavy Ion Test Planning and Analysis Have Been Completed.**

A custom radiation test board has been designed, fabricated and populated with components that will allow remote and continuous monitoring of voltages and currents to the CIS2521F device while it is being bombarded by heavy ions. The photo of the radiation test board is shown in Fig 15 below. We expect to complete the testing and analysis of the data before the end of 2018.

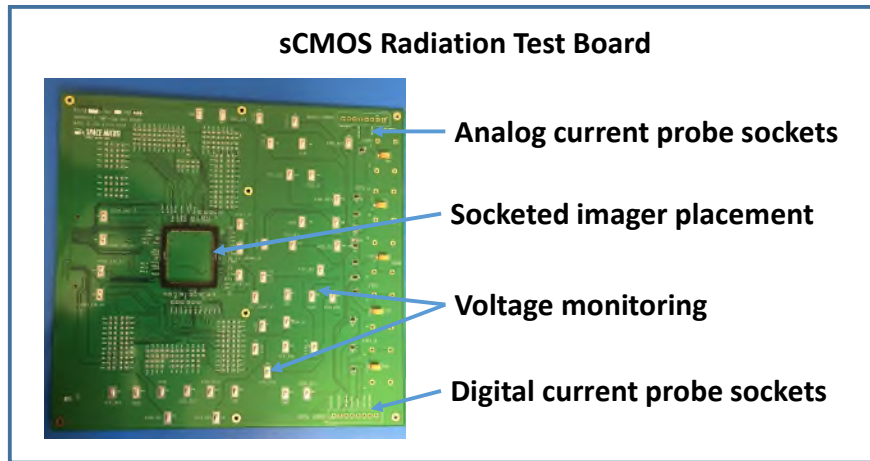


**Figure 15. Custom radiation test board for SEL and TID assessment**

## 7. CONCLUSIONS

Space Micro has evaluated several options for a next generation star tracker and space camera and we've concluded that a sCMOS based camera not only provides a significant improvement for star sensitivity and centroid accuracy but it also is a camera best suited for observation of dim space objects that reflect sunlight.

## 8. REFERENCES

1. CIS2521F Standard and Scientific Package Datasheet RevH, BAE Systems Imaging Solutions.
2. NOIH2SM1000A/D, HAS2 Image Sensor, On Semi January, 2015